

pubs.acs.org/acssensors Article

Toward Long-Term Accurate and Continuous Monitoring of Nitrate in Wastewater Using Poly(tetrafluoroethylene) (PTFE)—Solid-State Ion-Selective Electrodes (S-ISEs)

Yingzheng Fan, Yuankai Huang, Will Linthicum, Fangyuan Liu, André O'Reilly Beringhs, Yanliu Dang, Zhiheng Xu, Shing-Yun Chang, Jing Ling, Bryan D. Huey, Steven L. Suib, Anson W. K. Ma, Pu-Xian Gao, Xiuling Lu, Yu Lei, Montgomery T. Shaw, and Baikun Li*



Cite This: ACS Sens. 2020, 5, 3182-3193



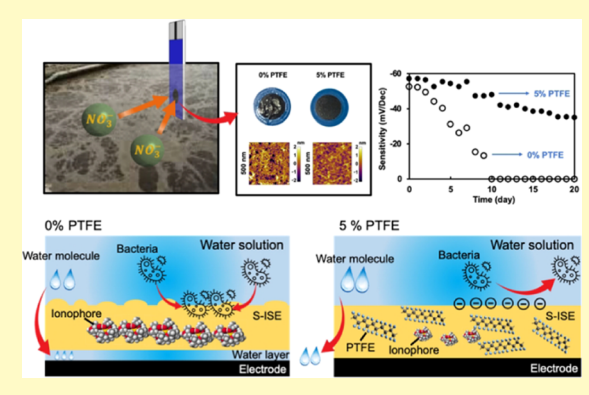
ACCESS

III Metrics & More

Article Recommendations

s Supporting Information

ABSTRACT: Long-term accurate and continuous monitoring of nitrate (NO_3^-) concentration in wastewater and groundwater is critical for determining treatment efficiency and tracking contaminant transport. Current nitrate monitoring technologies, including colorimetric, chromatographic, biometric, and electrochemical sensors, are not feasible for continuous monitoring. This study addressed this challenge by modifying NO_3^- solid-state ion-selective electrodes (S-ISEs) with poly-(tetrafluoroethylene) (PTFE, $(C_2F_4)_n$). The PTFE-loaded S-ISE membrane polymer matrix reduces water layer formation between the membrane and electrode/solid contact, while paradoxically, the even more hydrophobic PTFE-loaded S-ISE membrane prevents bacterial attachment despite the opposite approach of hydrophilic modifications in other antifouling sensor designs. Specifically, an optimal ratio of 5% PTFE



in the S-ISE polymer matrix was determined by a series of characterization tests in real wastewater. Five percent of PTFE alleviated biofouling to the sensor surface by enhancing the negative charge (-4.5 to -45.8 mV) and lowering surface roughness (R_a : 0.56 ± 0.02 nm). It simultaneously mitigated water layer formation between the membrane and electrode by increasing hydrophobicity (contact angle: 104°) and membrane adhesion and thus minimized the reading (mV) drift in the baseline sensitivity ("data drifting"). Long-term accuracy and durability of 5% PTFE-loaded NO_3^- S-ISEs were well demonstrated in real wastewater over 20 days, an improvement over commercial sensor longevity.

KEYWORDS: poly(tetrafluoroethylene), NO₃⁻ S-ISEs, wastewater, long-term accuracy and durability, antifouling, reading (mV) drifting, negative charge, surface roughness

ong-term accurate and continuous monitoring of nitrate (NO_3^-) concentration in wastewater and groundwater is critical to provide real-time information determining treatment efficiency and contaminant trend over time. Different types of nitrate monitoring technologies have been developed, including colorimetric, chromatographic, biometric, and electrochemical sensors. Nevertheless, colorimetric sensors are typically single use, such as a Griess colorimetric chip nitrate sensor, and hence are not feasible for continuous monitoring.² Chromatographic sensors (e.g., UV spectrophotometry) are complicated due to the requisite pretreatment of water samples and also cannot be used for real-time in situ monitoring.³ Biosensors such as copper-containing nitrate reductase (Cu-NIR) and viologen-modified sulfonated poly-(aminopropylsiloxane) (PAPS-SO₃H-V)^{4,5} usually have high selectivity for nitrate, but the short life span of microbial cells and enzymes makes them unfeasible for continuous monitoring in wastewater. Therefore, electrochemical sensing

techniques including impedimetric, voltammetric, and potentiometric methods have received high attention in the past two decades, due to their excellent accuracy, sensitivity, selectivity, and relatively simple configuration. Nevertheless, impedimetric detection methods (e.g., ion-imprinted, polymer-coated impedimetric nitrate sensor) require voltage stimulation to the electrodes, usually requiring high electric power. Voltammetric sensors are mostly suitable for clean water samples, as the signals can be severely influenced by impurities in wastewater under continuous potential scanning, largely limiting their real-world application. The accuracy of an

Received: July 10, 2020 Accepted: September 16, 2020 Published: September 16, 2020





amperometric sensor such as graphene oxide (GO)-modified amperometric nitrate sensors has not met the requisite standard (<5% deviation) due to severe reading drift at a fixed potential in wastewater and again is incompatible with real-time in situ continuous monitoring.⁸

In contrast, ionophore-based solid-state potentiometric ionselective electrodes (S-ISEs) overcome these shortcomings due to their high selectivity to the analyte (nitrate in this case) of interest, the ability to detect low concentration (\sim 55 μ g N/L), no requirement for an external power source, ease of use (just measure the potential (mV) difference between the working electrode and reference electrode), fast response (<2-10 s), low cost (<\$20 per sensor node, based on the sensor material cost), and miniature dimension (sensor diameter <2-10 mm). 9-13 However, two main problems remain, which are the focus of this work: lack of long-term accuracy and poor durability have constrained the solid-state ISEs for continuous monitoring in wastewater. To enhance long-term accuracy of water sensors, reading drift of the electrode signals (e.g., mV, mA, and Ω) must be fundamentally solved, especially for electrodes immersed in wastewater containing large amounts of inorganic/organic contaminants and/or microbial cells. Some progress has been made to alleviate electrode reading drift by adding an intermediate ion-to-electron layer, such as multiwalled carbon nanotubes (MWCNTs) or electropolymerized poly(3,4-ethylenedioxythiophene) (PEDOT), between the electrode (solid contact) and the S-ISE membrane polymer matrix. ^{14,15} However, the top ISE membrane layer exposed to the bulk wastewater solution suffers from fouling as a result of the adhesion of organic/inorganic compounds and/ or particles and thus acutely shortens useful life spans on the order of just a few hours or days for wastewater monitoring.¹ To enhance the durability of water sensors, nondispersive infrared (NDIR) nitrate sensors have been developed where organic/inorganic matter is periodically removed by cleaning, but this cleaning poses an obvious obstacle for long-term and continuous monitoring. To intrinsically alleviate bacterial attachment instead, the hydrophilicity of sensor surfaces could be enhanced. For example, graphene oxide on SiO₂ (GO-SiO₂) nanoparticles (NPs) have been used on a sensor surface due to their outstanding hydrophilicity to repel hydrophobic biofoulants. 18 Poly(ethylene glycol) (PEG), one of the most common hydrophilic polymers, was also combined with Al₂O₃ to photomodify the sensor surface via UV irradiation technique for antifouling. 19 Hydrophilic ionselective electrode (ISE) normally contains water (0.6 mol/ dm³).²⁰ However, high water uptake/sorption can constitute a major drawback after sensors are immersed in water solution for a long period of time, since this will lead to water accumulation between the ISE membrane and electrode (solid contact) and eventually cause reading (mV) drifting.

In this study, the long-term accuracy and durability of NO_3^- S-ISEs for continuous wastewater monitoring were improved, based on both reducing water layer formation between the membrane and electrode (solid contact) and alleviating sensor surface fouling. Specifically, the chemical modification of the S-ISE membrane polymer matrix by mixing with poly-(tetrafluoroethylene) (PTFE, $(C_2F_4)_n$), a hydrophobic polymer, ²¹ could optimize two properties—the water repellency of the S-ISE polymer matrix (to reduce water layer formation between the membrane and electrode) and the antifouling sensor surface (to prevent bacterial attachment). PTFE has already been used for resistive tactile- and catalytic-type H_2

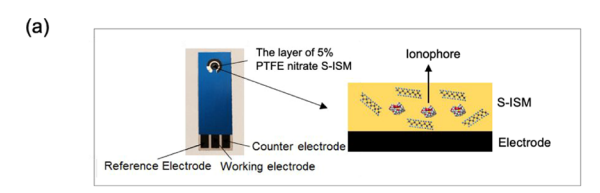
sensors to resist high temperature (180 °C)²² and corrosion.²³ For the novel nitrate S-ISEs presented herein, PTFE particles are expected to enhance the adhesion of the S-ISE membrane, mitigate the formation of water layer between the sensing membrane and electrode, and solve reading (mV) drift. Furthermore, as a highly negatively charged polymer (ζ potential of PTFE: -43.7 mV),²⁴ PTFE could improve the negative charge of the S-ISE polymer matrix, effectively repelling negatively charged bacteria from attaching onto the sensor surface. PTFE was also found to elevate the surface smoothness of the electrode surface, 25 which might aid in alleviating the membrane fouling in wastewater. In this study, PTFE has been mixed into the S-ISE polymer matrix covering a wide range of practical proportions. By examining the accuracy, sensitivity, and durability of these NO₃ S-ISEs in real wastewater, the optimal ratio of 5% is determined. Next, the mechanisms of PTFE to reduce water layer formation between the membrane and electrode are explored using optical transmittance, viscosity, adhesion, contact angle, and a water layer test. The mechanisms of PTFE to alleviate biofouling are also investigated using ζ potential, surface charge, and surface roughness. Ultimately, the long-term accuracy and durability of our PTFE-loaded nitrate S-ISEs are compared side by side with conventional nitrate S-ISEs as well as commercial nitrate sensors in real wastewater over 20

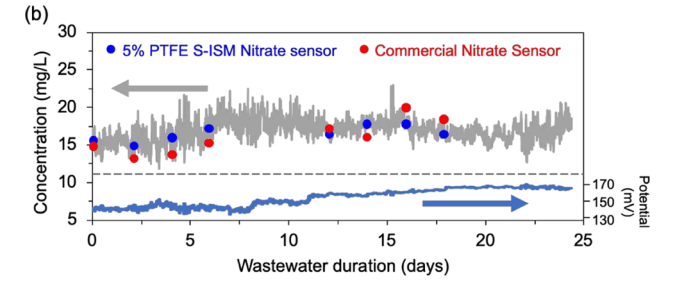
■ EXPERIMENTAL SECTION

Fabrication and Calibration of NO₃⁻ Solid-State Nitrate S-ISEs with Different PTFE Ratios. The sensor support (length: 3.5 cm, width: 1.5 cm, thickness: 0.1 cm, aerial view of the sensor support: Figure 1a; cross-sectional image of the sensor support: Figure S1) was fabricated by the conventional screen printing technology (SPT) (eDAQ, ET083). The NO₃⁻ ISE membrane mixture consists of nitrate ionophore VI (9-hexadecyl-1,7,11,17tetraoxa-2,6,12,16-tetraazacycloeicosane, Sigma-Aldrich), plasticizer dibutyl phthalate (DBP, Sigma-Aldrich), tetraoctylammonium chloride (Sigma-Aldrich, served as anion exchanger), and poly(vinyl chloride) (PVC, high molecular weight, Sigma-Aldrich). DBP and PVC act as the supporting materials for ionophore and form a homogeneous phase in the ISE mixture. Subsequently, poly-(tetrafluoroethylene) (PTFE) particles at different ratios (0, 2.5, 5, 7.5, and 10% w/w) were individually added into this mixture. Because PTFE particles are insoluble in this plasticized PVC, PTFE was dispersed in the ISE membranes presented in this work. The percentages of all components for these five distinct membranes are shown in Table S1. The mixture was dissolved in 400 µL of tetrahydrofuran (THF) and then fully mixed ultrasonically for 10-15 min. Fifteen microliters was next carefully drop-cast onto the surface of the carbon-based working electrode (radius: 2.5 mm) (Figures 1a and S1). The liquid ISE membrane on the electrode was dried at room temperature over 48 h under N2 and a lightless environment to form the solid-state ISE (S-ISE).

For sensor calibration, the NO_3^- S-ISE sensors with different PTFE ratios (0, 2.5, 5, 7.5, and 10%) were individually submerged into the water solution (100 mL) of 1 mg N/L KNO₃ (0.07 M) continuously stirred at 100 rpm via a Thermolyne Cimarec-top stirring plate. The nitrate concentration solution was sequentially increased from 2, 4, 8, 16, 32 to 64 mg N/L every 50 s by adding a concentrated KNO₃ solution. The readings (mV) of the NO_3^- S-ISEs were individually recorded at 0.1 s intervals using a multichannel electrochemical workstation (CHI 660D potentiostat).

Continuous Long-Term Stability and Accuracy Test of NO₃⁻ S-ISEs in Wastewater. The long-term stability and accuracy of NO₃⁻ S-ISEs with 0 and 5% PTFE were examined by immersing multiple sensors of each type into parafilm sealed beakers containing wastewater (the UConn Wastewater Treatment Plant (WWTP)





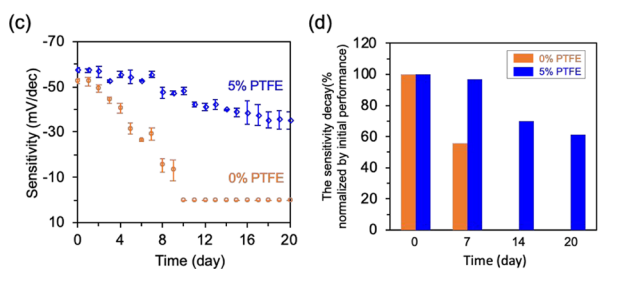


Figure 1. (a) Schematic illustration of PTFE-loaded nitrate (NO_3^-) S-ISEs alongside an actual assembled sensor. (b) Long-term real-time potential (mV) readings of the optimized 5% PTFE nitrate (NO_3^-) S-ISE (blue line) and the calculated concentration (mg/L) of the S-ISE (gray line and blue dots) in real wastewater over 20 days and comparison with a commercial nitrate sensor (red dots). (c) Comparison of long-term sensitivity between the 5 and 0% PTFE NO_3^- S-ISEs over 20 days. (d) Sensitivity decay (%, normalized by the initial performance) of the 5 and 0% PTFE NO_3^- S- ISEs over 20 days.

effluent (Table S2)) for 24 days. Three pieces of NO₃⁻ S-ISEs with 0% PTFE loading, and three pieces with 5% PTFE-loaded, were briefly removed from the wastewater daily and calibrated at the sequentially increasing NO₃⁻ concentrations via concentrated KNO₃ (2, 4, 8, 16, 32, and 64 mg N/L). In this manner, the long-term sensitivity of these sensors (mV/dec of [NO₃⁻]) could be determined throughout the 24 day period. The potential readings (mV) of all NO₃⁻ S-ISEs tested were individually recorded every 5 s using an electrochemical workstation (CHI 660D). Subsequently, all 345 600 potential readings (mV) per sensor were converted to nitrate concentration (mg/L) using the updated daily calibration curves and potential drifting (mV) regression results over 24 days. The commercial YSI nitrate sensor (model: Professional Plus) as the calibration device was validated by the dimethylphenol method (method 10206) using Hach DR2800 before every time usage.

Selectivity Coefficient Measurement of NO_3^- S-ISEs. The selectivity coefficient of NO_3^- S-ISEs is conducted by measuring the potential (mV) of NO_3^- S-ISEs with the absence and presence of nontargeted interfering ions (Cl⁻, $PO_4^{\ 3-}$, and $SO_4^{\ 2-}$). Specifically, a series of NO_3^- (primary ion) solutions (concentrations: 0.0085–8499.47 mg/L) are added incrementally to a distilled water solution without any interfering ions, and the potential (mV) readings of NO_3^- S-ISEs are recorded. Then, a series of interfering ion solutions (Cl⁻: 0.0058–5844 mg/L; $H_2PO_4^-$: 0.014–14196 mg/L (pH: ~7–4.7); and $SO_4^{\ 2-}$: 0.014–14204 mg/L) are added individually to the distilled water solutions without NO_3^- (primary ion) in an incremental mode, and the potential (mV) readings of NO_3^- S-ISEs are recorded under each type of ion solution and each concentration. After obtaining these calibration curves of NO_3^- S-

ISEs with the absence and presence of interfering ions, the selectivity coefficient is calculated by the separate solution method $(SSM)^{26-28}$

$$\log K_{A,B}^{\text{pot}} = \frac{(E_{B} - E_{A})z_{A}F}{RT \text{ In } 10} + \left(1 - \frac{z_{A}}{z_{B}}\right)\log a_{A}$$

where E_A and E_B are the primary and interfering ion potential values obtained from the same ion activity $(a_A = a_B)$ from the calibration curve, respectively, and z_A and z_B are the charges of two ions targeted.

Transmittance Measurement of the PTFE-Loaded NO₃⁻ S-ISE Polymer Matrix. The transmittance of the PTFE-loaded NO₃⁻ S-ISE polymer matrix is measured to characterize the aggregation of PTFE particles and any oversaturation of PTFE in the S-ISE polymer matrix. Here, the ISE membrane mixture solutions with different PTFE ratios (0, 2.5, 5, 7.5, and 10%) were directly drop-cast onto the surface of an ultraviolet-visible (UV-vis) cell before drying at room temperature over 24 h to form a solid-state ISE membrane. The transmittance of each S-ISE membrane is based on the optical transmittance of the assembled device minus that of the transparent substrate alone, according to an ultraviolet-visible (UV-vis) spectrophotometer (UV-2450, Shimadzu, Japan) across the wavelength range from 200 to 800 nm.

Viscosity Test of Liquid-State ISE Membrane and Adhesion Test of S-ISE Membrane. Steady shear viscosity data were collected at 25 °C using an AR-G2 rheometer (TA instrument, New Castle, U.K.) equipped with a solvent trap. A cone-and-plate test fixture with a diameter of 20 mm and a cone angle of 2° was used. Test samples for viscosity measurements were prepared by diluting 0.258 g of the polymer solutions (liquid-state membrane with 0 and 5% PTFE, respectively) with 0.258 g of THF. These samples were loaded within a truncation test gap of 50 μ m, and the apparent shear viscosity of the materials was then measured as a function of the increasing shear rate from 1 to 100 s⁻¹.

The adhesion of the S-ISE membrane was tested by using a transparent tape (Gorilla Tape) to tear up the membrane from the working electrode of the sensor support. Specifically, the tape was first firmly stuck onto the S-ISE membrane for 10 s and then rapidly pulled off from the membrane. The membrane would be teared up onto the tape if the adhesion of the membrane to the electrode is weak, while the membrane would stay on the electrode if the adhesion is strong. Four S-ISE sensor samples were examined, with two S-ISE sensors (0 and 5% PTFE) before immersion to water solution and two S-ISE sensors (0 and 5% PTFE) after immersion in water solution for 7 days.

Water Layer Test of NO₃⁻ S-ISEs for 7 Days. Water layer test has been commonly used as an indirect indicator to verify the formation of water layer on the electrode surface within several hours of immersion in water solution.^{27,28} Because long-term monitoring is targeted in this study, water layer test is conducted for 7 days. Specifically, the NO₃⁻ S-ISEs with 0 and 5% PTFE are first immersed in the NaNO₃ solution (0.1 M) containing primary target ion NO₃ for 72 h to achieve an equilibration with the condition solution. Subsequently, both sensors are immersed in a NaCl solution (0.1 M) containing an interfering ion (Cl⁻) for 24 h, which is long enough for ions to be transported through the membrane and equilibrate with the water layer formed beneath the membrane. Finally, both sensors are put back to the primary target ion solution (NaNO₃) and immersed for 72 h to equilibrate with the solution. The potential readings (mV) of both sensors are continuously recorded at an interval of 10 s using the electrochemical workstation (CHI 660D).

Surface Charge Measurement NO_3^- S-ISE Surface, ζ Potential, and Particle Size Measurement of PTFE Powder. The surface charge of the S-ISE surface is measured by the streaming current method using an electrokinetic analyzer (SurPASS Anton Paar, Austria). The S-ISE membrane samples are cut into 0.2 cm \times 0.1 cm pieces and then immobilized on an adjustable gap cell. A KCl solution (1.0 mmol/L) is used as the background electrolyte for determining the ζ potential. In addition, hydrochloride (HCl) and potassium hydroxide (KOH) are used to adjust the pH value.

ACS Sensors Article pubs.acs.org/acssensors

Subsequently, the surface charge of the S-ISE surfaces at different pH levels is calculated (Visolab for SurPASS software).

Additionally, the surface charge of PTFE-free S-ISE membranes at different nitrate concentrations (NaNO₃, 0.2, 1, 2, 4, 8, and 16 mM) is measured by the streaming current method using an electrokinetic analyzer (SurPASS Anton Paar, Austria)²⁹ to determine whether nitrate concentration affects the surface charge of the ISE membrane. Before the test, PTFE-free S-ISE membranes are immersed in different nitrate concentrations (NaNO₃, 0.2, 1, 2, 4, 8, and 16 mM) for 48 h. 30,31 Then, the S-ISE membrane samples are cut into 0.2 cm × 0.1 cm pieces and immobilized on an adjustable gap cell. NaNO₃ solutions of different concentrations (0.2, 1, 2, 4, 8, and 16 mM) are used as the background electrolyte (pH: ~7.0) for determining the surface charge.

 ζ potential distributions of PTFE particles are determined via laser Doppler anemometry using a ZetaSizer Nano-ZS system (Malvern, U.K.). 32 Around 1.5 mg of PTFE particles is dispersed in 1 mL of 0.1 mM sodium chloride and 0.01 mM (pH: 7) solution of Tween 80 in ultrapure water (Synergy system, Millipore). Sodium chloride (NaCl) is added to ensure an adequate and reproducible electroconductivity in the continuous phase to reduce uneven electric field distortions. Tween 80, a nonionic surfactant, is used to ensure complete dispersion of the hydrophobic particles in water. PTFE particles are further diluted as needed and transferred to disposable folded capillary ζ cells for analysis. Such ζ cells are subjected to an electric field for microelectrophoresis, in which particle velocity is measured via phase analysis light scattering at 25 °C (n = 3 and 20 measurements per replicate). This particle velocity is related to the surface charge of PTFE particles, which is used to determine the electrophoretic mobility and ζ potential.³³

The size distribution of PTFE powders was characterized using a field-emission scanning electron microscope (SEM, FEI TeneoLo-Vac) at an accelerating voltage of 10.0 kV (Figure S2). Specifically, the PTFE powders were cast onto the copper conducting tape and installed on the sample stage for SEM imaging. The average size of PTFE particles was calculated by measuring 50 particles in the obtained SEM images using the FIJI (ImageJ) software.

Surface Roughness Measurement of NO₃⁻ S-ISE Surface. Topography images of relatively smooth areas on the ISE membranes are acquired utilizing a Cypher VRS Asylum Research atomic force microscope (AFM). The instrument is operated with an OMCL-AC160TS probe (nominal 7 nm radius of curvature and 40 N/m spring constant) in AC mode, as previous work suggests that contact mode imaging can penetrate PVC sample surfaces.³⁴ Both the S-ISE membranes with 0 and 5% PTFE samples are scanned over 5 μ m and 500 nm dimensions, all with 512×512 pixels per image. The statistics (average and standard error) for each sample is calculated based on the arithmetic average roughness (Ra) and skewness values from 15 representative 500 nm × 500 nm regions and is tested for statistically significant differences through t-tests.

Electrochemical Analysis and Contact Angle Measurement of NO₃ - S-ISEs. Electrochemical impedance spectroscopy (EIS) is performed to characterize the variation of the electrochemical properties of the 0 and 5% PTFE-loaded S-ISEs in wastewater over time. The measurements are conducted in 0.1 M KCl solution. The results are recorded in the frequency range from 100 kHz to 0.1 Hz by using an excitation amplitude (ΔE_{ac}) of 10 mV before and after a 20 day immersion in wastewater. Data was fitted based on the equivalent circuit models in ZSimpWin software. In addition, the hydrophobicity of the S-ISE surfaces with 0 and 5% PTFE was examined by measuring the contact angle using a CAM 101 optical surface tension meter (KSV Instrument Inc.) as previously reported.³

S-ISE Membrane Morphology Observation and Thickness Measurement. The morphology of the S-ISE membrane surface and the thickness of the S-ISE membrane before and after immersion (20 days) in wastewater were characterized using an SEM (FEI TeneoLoVac) at an accelerating voltage of 10.0 kV. Specifically, the membranes (0 and 5% PTFE) along with the sensor supports were cut into semicircle-shaped samples (radius: 2.5 mm) to generate a cross-sectional view field. These semicircle-shaped cross-sectional

samples were then adhered onto copper conducting tapes and fixed at the side of the sample stage to allow the cross-sectional view of the samples under the SEM.

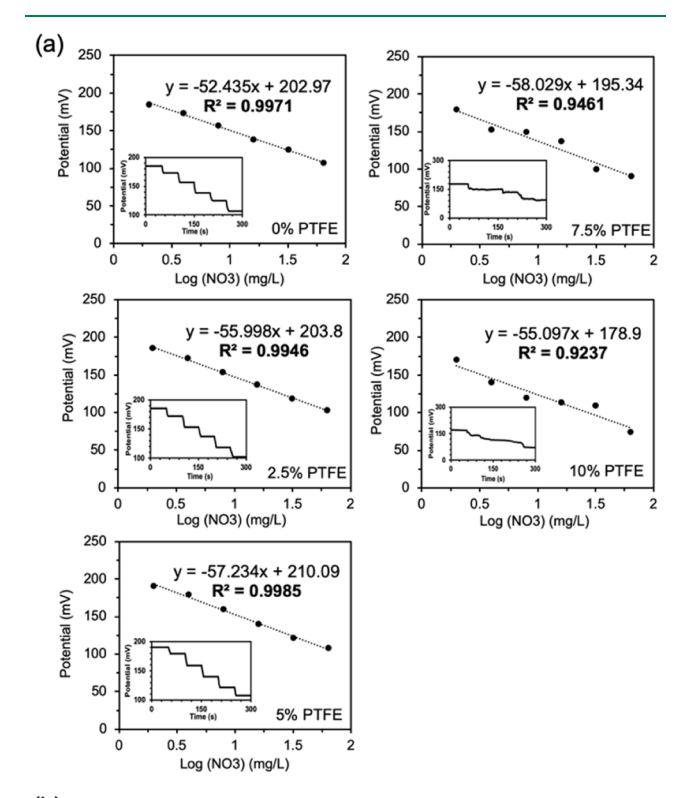
RESULTS AND DISCUSSION

Comparison of PTFE-Loaded NO₃⁻ S-ISE with Commercial Sensor in Terms of Accuracy and Continuous Monitoring. Figure 1 compares the performance of our PFTE-loaded nitrate S-ISEs, ultimately optimized with a PTFE ratio of 5%, alongside a commercial nitrate sensor (Professional Plus Multiparameter Instrument equipped with nitrate probes, YSI Co.). This assessment is based on continuous monitoring, as well as long-term accuracy testing, during more than 24 days of operation in real wastewater ($[NO_3^-]$: 15–18 mg/L) collected from the UConn WWTP. The potential readings (mV) of all of the NO₃⁻ S-ISEs tested were individually recorded every 5 s (Figure 1b, blue line) and then converted to the concentration readings (mg/L) (Figure 1b, gray line) using the updated daily calibration curves/slopes and the potential (mV) drift regression results over 24 days. The concentration readings of the PTFE-loaded nitrate S-ISE were steady in wastewater throughout the 24 day test period (Figure 1b). The accuracy was examined by selecting eight points (blue dots in Figure 1b) and verifying with the nitrate commercial sensor as the one-point calibration device (red dots in Figure 1b). The discrepancy was less than 5% throughout the test period. The commercial YSI nitrate sensor was unable to continuously monitor wastewater even for 20-30 min, suffering from severe fluctuation and reading drifting (red line in Figure S3) mainly due to the biofouling, and had to be taken out from wastewater every 30 min for cleaning by manually paper-wiping sensor surface, meaning that the monitor could only be used as an intermittent one-point measurement device and/or a calibration device for wastewater monitoring. In addition, the accuracy of the commercial nitrate sensor as a calibration device was verified by comparing the sensor readings with the standard dimethylphenol method (method 10206) during a 2 h period (Figure S4). The difference was less than 1.5%, meaning that the commercial sensor is a reliable calibration device in this study.

The periodically measured sensitivity (mV/dec of $[NO_3^-]$) with the PTFE-loaded S-ISEs also exhibited excellent stability throughout the 24 day test, starting at -58 mV/dec of concentration and ending better than -35 mV/dec on the 20th day (Figure 1c). The sensitivity of the nitrate S-ISEs without PTFE dropped from −52 to 0 mV/dec after 10 days in wastewater, meaning that it had reached its life span and needed replacement. In addition, PTFE-loaded S-ISEs outperformed the commercial nitrate sensors, which could only last for 30 min in wastewater, and similarly are better than the specifications for other types of nitrate sensors such as nondispersive infrared (NDIR) nitrate sensors, imprinted polymer impedimetric nitrate sensors, and selective enzymatic nitrate sensors. 6,17,36 We hypothesize that there are two main reasons for the particularly superior performance of the PTFEloaded S-ISEs. First, the PTFE mixed with the PTFE-loaded S-ISE membrane polymer matrix greatly enhances the antifouling capability by modifying the sensor surface charge²⁹ and the surface topography.³⁷ Second, the enhancement of adhesion of the PTFE-loaded membrane reduces the water formation between the S-ISE membrane and electrode (solid contact) interface and assures long-term accuracy for continuous monitoring. The remainder of this work confirms these

assumptions, but to put it into context, Figure 1d recasts some of the data from Figure 1c at benchmark time points and now displays the percent degradation in sensitivity as normalized by the initial performance. The PTFE-loaded nitrate S-ISEs exhibited perfect stability over 1 week, which ultimately diminished less than 40% over 20 days. The 0% PTFE S-ISEs degraded almost linearly in less than 2 weeks (Figure 1d). Once again, though, these tests are performed in wastewater, i.e., a substantially more challenging condition than clean water, which has been often used instead for sensitivity benchmarking.

Determination of Optimal PTFE Ratio in the S-ISE Polymer Matrix. To determine the optimal PTFE ratio in the S-ISE membrane polymer matrix, the NO₃⁻ S-ISEs with different PTFE ratios (0, 2.5, 5, 7.5, and 10%) were examined in nitrate solutions ranging between 1 and 64 mg/L (Figure 2a), i.e., spanning typical nitrate concentrations for municipal



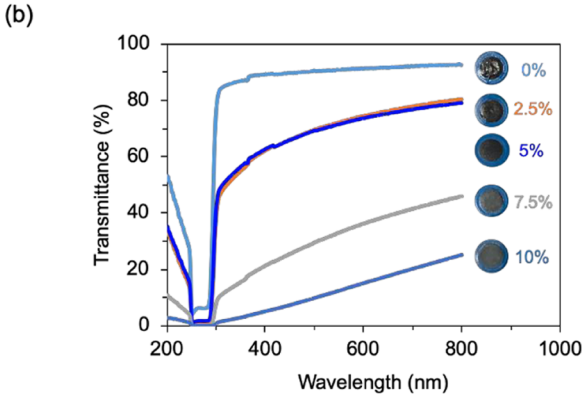


Figure 2. (a). Calibration curve of NO_3^- S-ISEs with different PTFE ratios (0, 2.5, 5, 7.5, and 10%). (b). Optical transmittance of NO_3^- S-ISEs with the same PTFE ratios across the spectrum from 200 to 800 nm.

wastewater. 38,39 According to the Nernst equation $E=E^0+\frac{2.3026\times RT}{zF}\log(aI)$, a near-ideal Nernstian slope (58 mV/dec) was achieved for $\mathrm{NO_3}^-$ S-ISEs with medium PTFE ratios of 5 and 7.5%. The most linear response, though ($R^2>0.99$, where R^2 is the standard statistical measure of the closeness of the data to the fitted regression model), was observed for 0, 2.5, and 5% PTFE samples, indicating the best accuracy for these lower PTFE ratios. The sensor with the PTFE ratio of 5% therefore exhibited the best performance, in terms of slope, and also accuracy with an R^2 value of 0.9985. Notably, this is higher than nitrate sensors reported elsewhere, including polypyrrole/glassy carbon electrode (PPy/GCE) electrochemical nitrate sensors ($R^2=0.9867$) and extendedgate type nitrate sensors ($R^2=0.9867$) and extendedgate type nitrate sensors ($R^2=0.98$).

Interestingly, once the PTFE ratio increased to 7.5 or 10%, the R^2 values dropped to 0.9461 and 0.9237, respectively, indicating that the sensor linearity was sacrificed. In addition, compared with the residual mean standard deviation (RMSD) value (2.18 mV) of the PTFE ratio of 5%, the RMSD of the PTFE ratio of 7.5 and 10% increased to 7.12 and 8.14 mV, respectively, exhibiting that 5% PTFE ratio possessed the smaller expected error of the measurement for the regression line. This superior linearity of the 5% PTFE-loaded NO₃⁻ S-ISEs (R²: 0.9985, RMSD: 2.18 mV) still exhibited a slight deviation (\sim 8%) when converted from log(concentration) to concentration, but it is acceptable given a typical measurement error ranging from 5 to 10% in wastewater monitoring. We surmise that this could result from aggregation of PTFE particles and hence oversaturation of PTFE in the S-ISE membrane polymer matrix. The particle size of the PTFE powder was measured as 125 ± 18.59 nm based on the SEM images analysis (Figure S2). In addition, when the ISE membrane surface was magnified a thousand times, some acicular crystals were observed on the 0% PTFE ISE membrane surface (Figure S5a), which was assumed to result in a rough surface. In contrast, when the PTFE ratio was 5%, the ISE membrane became smooth and PTFE particles were evenly dispersed in the membrane (Figure S5b), which improved the PVC film-forming property and solubility. Subsequently, the acicular crystals formed again when the PTFE ratio was increased to 10% in the ISE membrane (Figure S5c), undermining the sensor property.

The necessary uniformity of these PTFE and S-ISE composites therefore diminished at high PTFE ratios, which will furthermore degrade the physical and mechanical properties. 41 Such PTFE agglomeration was confirmed by UV-vis transmittance measurements at 25 °C (Figure 2b). The transmittance of the NO₃⁻ S-ISEs was better than ~40-80% across the visible light spectrum (300-800 nm) for low PTFE ratios (0-5%), while the transmittance dropped to 0-45% for higher PTFE ratios (7.5 and 10%). This oversaturated PTFE (>5%) aggregated within the membrane, blocked the light transmittance, and concomitantly impaired the S-ISE accuracy. Furthermore, the selectivity coefficient (K_{AB}^{pot}) of NO_3^- S-ISE was determined using the separate solution method (SSM). A low value of $K_{A,B}^{pot}$ indicated a strong preference of the electrode for the primary ion to the interfering ion. The selectivity coefficients of 5% PTFE S-ISEs ($log K_{NO_3^-,Cl^-}^{pot}$: -2.06, $\log K_{{\rm NO_3}^-,{\rm H_2PO_4}^-}^{\rm pot}$: -2.80, $\log K_{{\rm NO_3}^-,{\rm SO_4}^2}^{\rm pot}$: -2.83) were comparable to those of 0% PTFE S-ISEs ($\log K_{\mathrm{NO_3}^{-},\mathrm{Cl}^{-}}^{\mathrm{pot}}$ of -2.14, $\log K_{\text{NO}_3^-,\text{H},\text{PO}_4^-}^{\text{pot}}$ of -2.89, $\log K_{\text{NO}_3^-,\text{SO}_4^{2-}}^{\text{pot}}$ of -2.95; Figure S6),

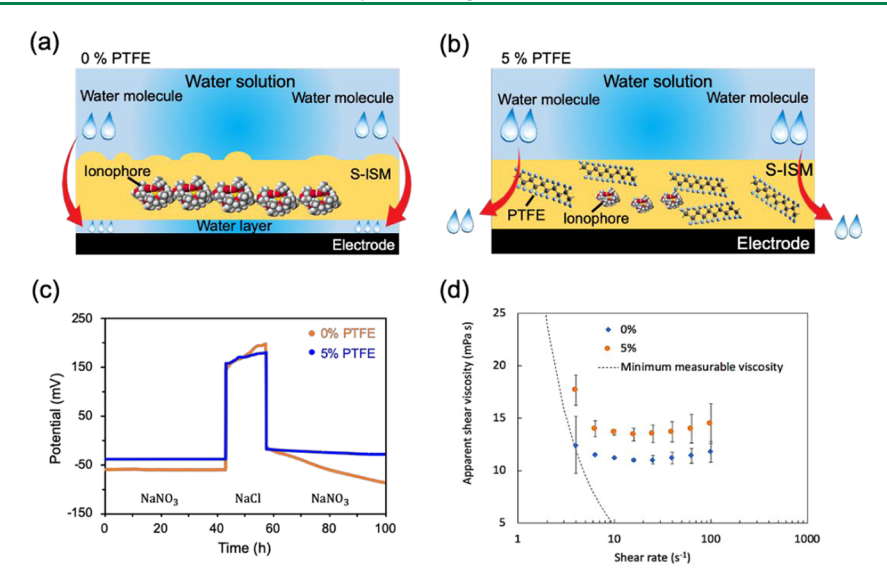


Figure 3. (a) Diagram of water invasion to the interface between the S-ISE membrane polymer matrix and electrode surface with 0% PTFE and (b) diagram of no such water invasion for 5% PTFE. (c). Comparison of the long-time water layer test based on potential (mV) drift when changing ions in the solution, for the NO₃⁻ S-ISEs with 0 and 5% PTFE. (d) Apparent shear viscosity as a function of shear rate for 0 and 5% PTFE. (The error bar represents the standard deviation from two separate measurements on the same sample).

indicating that 5% PTFE-loaded nitrate S-ISEs possessed superior selectivity over interfering ions. Therefore, the optimal ratio of 5% PTFE in the S-ISE membrane polymer matrix was selected for all further investigations due to its balanced superior sensitivity, accuracy, and selectivity.

Reduction of Water Layer Formation between the Membrane and Solid Contact Using PTFE. The accuracy of S-ISE for continuous monitoring in wastewater can suffer from reading (mV) drifting caused by water layer formation between the S-ISE membrane polymer matrix and the electrode surface, 42,43 as sketched in Figure 3a. In contrast, the PTFE-loaded S-ISE was expected to mitigate the water layer formation between the S-ISE membrane and electrode surface (Figure 3b). Water layer tests were thus performed to assess such water layer formation for the S-ISE membrane after immersing alternately in NaNO3 and NaCl solutions for 7 days.²⁸ The presence of a water layer was expected to cause a potential (mV) drift during this solution change.²⁰ Here, the NO₃ S-ISE with 0% PFTE exhibited a strong positive potential drift (mV) of ~54 mV when changing from the solution containing NO₃⁻ to the solution containing Cl⁻ (Figure 3c) and then a negative potential drift also of ~70 mV when returning from Cl⁻ back to NO₃⁻. On the contrary, the NO₃⁻ S-ISE with 5% PTFE exhibits a more stable potential (mV) (~20 mV) when switching between the solutions over the same time scale (72-24-72 h). In fact, the result (0.9)mV/h) is comparable to previous water-repellent studies using a much more complex configuration of graphene as the solid contact, a poly(3-octylthiophene-2,5-diyl) (POT) coating, and a silicon rubber-based poly(acrylate) ISE membrane. 44–46 This negligible water layer formation (Figure 3b) could be ascribed to the enhancement of the PTFE-loaded S-ISE adhesion with the electrode surface, which is validated by the adhesion tape test (tearing the S-ISE membrane from the electrode using a scotch tape; Figure S7a). Before immersing into the water solution, S-ISE membranes with 0 and 5% PTFE adhered quite firmly on the electrode surface and cannot be teared up using the tape. However, after immersing into the water solution for 7 days (the same time scale as the water layer test), the 0%

PTFE S-ISE membrane adhered loosely on the electrode surface and could be wholly teared up by the tape, while the 5% PTFE S-ISE membrane was still firm on the electrode surface and adhered tightly and nearly kept its intactness during the adhesion tape test. Further, the viscosity measurement results revealed that for the same (1:1) dilution with THF, the ISE mixture containing 5% of PTFE had a higher viscosity compared to the sample without PTFE (Figure 3d). The minimum measurable viscosity based on the low-torque limit of rheometer was calculated and included in the data plot as a dotted line (Figure 3d). Inclusion of PTFE increased the viscosity of the polymer layer, which may have impeded the water layer formation and suppressed membrane deformation.

Furthermore, the enhancement of hydrophobicity is validated by the measured water contact angle of the S-ISEs with 5% PTFE S-ISEs (105°), while it is only 77° for the S-ISEs with 0% PTFE (Figure S7b). However, contact angles are often affected by surface roughness. To eliminate the influence of the surface roughness on the S-ISE membrane, the relationship between roughness and contact angle is applied here based on the Wenzel principle 50,51 (eq 1 (contact angle <90°) and eq 2 (contact angle >90°))

$$\cos \theta^* = r' \cos \theta \tag{1}$$

$$\cos \theta^* = r'f \cos \theta + f - 1 \tag{2}$$

where θ^* is the measured contact angle; θ is the contact angle with the smooth surface; f is the proportion of the actually wetted surface; and r' is the roughness coefficient (77°: 1.612, 105°: 2.517), which is the ratio of the size of the overall surface to the surface projected geometrically onto a plane. Based on eqs 1 and 2, the contact angle of 0% PTFE S-ISEs with the total smooth surface is advanced to 82°, and the 5% PTFE-containing S-ISEs with the total smooth surface are receded to 96°.

Effect of PTFE on S-ISE Surface Charge and Surface Roughness. The surface charge of the S-ISE membrane polymer matrix directly affects the sensor long-term durability in real wastewater since electrostatic repulsive forces between

the charged surface and typically negatively charged microbial cells in the wastewater could prevent the sensor surface fouling. ^{29,52} Although bacteria in wastewater differ for their outermost surfaces due to variations in the chemical or physical structure, basically all bacteria as well as other natural surfaces carry a net negative charge. ^{52,53} For example, the ζ potential of *Paenibacillus polymyxa* bacteria sustained around –40 mV at pH ranging from 4 to 10^{54} and the ζ potential of *Escherichia coli* could reach up to -47.8 mV at pH $8.4.^{55}$ Here, the NO₃⁻ S-ISEs with 5% PTFE exhibited a higher negative surface charge (-4.5 to -45.8 mV) than that with 0% PTFE (22.1 to -25.9 mV) across the pH range from 2 to 10 (Figure 4). This is attributed to a ζ potential for PTFE as low as -43.7

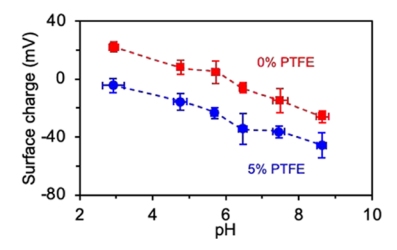


Figure 4. Surface charge of the NO₃⁻ S-ISE surface with 0 and 5% PTFF.

mV at pH 7 (Figure S8a), which results from the PTFE backbone ($(C_2F_4)_n$) being completely encased in fluorine atoms (Figure S8b), i.e., the most electronegative element at 3.98 on the Pauling scale.²⁴ Other previous studies examining antifouling, based on hydrogels containing negatively charged 3-sulfopropyl methacrylate potassium salts, found ζ potentials of only -3-1 mV for pH $7.4.^{56}$ Negative copolymer coatings have also been considered to enhance antifouling, resulting in ζ potentials between 0 and -30 mV in water for pH values ranging from 1 to $10.^{57}$ The much stronger electrokinetic repulsion of negatively charged microbial cells in wastewater by our NO_3^- S-ISEs with 5% PTFE helps explain our excellent antifouling performance.

Besides PTFE, nitrate concentration could be another factor influencing the surface charge of the S-ISE membrane. To determine such an effect, the surface charge of the S-ISE membrane with 0 and 5% PTFE was measured in solutions of different nitrate concentrations (NaNO $_3$) (0.2, 1, 2, 4, 8, and 16 mM) at the unadjusted pH (\sim 7.0) (Figure S9). The surface charge of both S-ISE membranes increased with nitrate

concentrations (0.2–4 mM) and then stabilized at high nitrate concentration (8–16 mM) (Figure S9a,b). However, nitrate concentration nearly had no impact on the selectivity variation in the water solution over time (Figure S9c,d), though the selectivity of the S-ISE membrane with 0% PTFE declined much faster than that with 5% PTFE. This result essentially excluded the possibility of nitrate concentration affecting the ISE membrane property and further validated the effective enhancement of the S-ISE membrane antifouling capability by PTFE-containing and varying the sensor surface charge.

Along with changing the charge at the sensor surface, PTFE incorporation is also found to diminish the surface roughness, another critical factor for limiting bacterial adhesion. 33-36 For instance, bacteria have been found to be more likely to be attached and entrained onto a rough surface than smooth membrane surfaces.³⁷ Such biofouling could result in the blockage of ion penetration into the sensor entity, leading to reading drifting (mV) and/or deteriorating accuracy. 62 Accordingly, the roughness was calculated based on topography measurements acquired using an atomic force microscope (AFM), which has elsewhere been demonstrated to be effective in investigating nanocomposite membrane performance for desalination. 63 Figure 5 displays the representative topography images for both S-ISEs with 0 and 5% PTFE specimens. Images of both samples at the 5 μ m range (Figure S10a,b) exhibit occasional protruding features (bright) with effective diameters ranging from 50 to as much as 1500 nm. The nanostructure in between these structures is the most important difference between the samples for ion sensing, though, as evidenced by the higher-magnification 500 nm scans (Figure S10c,d). Specifically, the pores on the 0% PTFE S-ISE membrane sample are deeper, while the 5% PTFE S-ISE membrane sample appears to have finer pores as well as microstructural features suggestive of domains or grains and their interfaces. In addition to these visual distinctions, the arithmetic average roughness (R_a) based on the data from 15 regions (Table S3) for the 0% PTFE S-ISE membrane was statistically greater than 15 regions for the 5% PTFE S-ISE membrane (0.69 \pm 0.05 and 0.56 \pm 0.02 nm for 0 and 5% PTFE S-ISE membranes, respectively, with p = 0.015) (Figure 5a). Compared with antifouling poly(vinylidene fluoride) (PVDF)/graphene oxide (GO) ultrafiltration membranes $(R_a: 40.8 \text{ nm})^{64}$ and GO-TiO₂/PVC mixed-matrix antifouling membranes (R_a : 29.1 nm),⁶⁵ the much smaller R_a value (0.56 nm) of the 5% PTFE S-ISE membrane represents a far

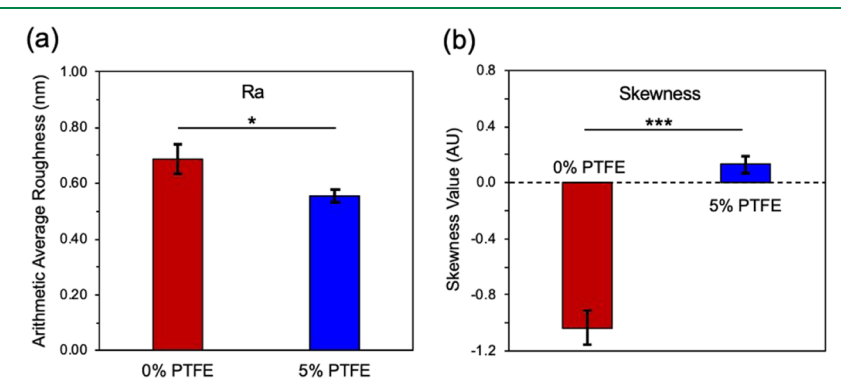


Figure 5. (a) Mean arithmetic average roughness (R_a) and (b) skewness values based on fifteen 500 nm × 500 nm locations on 0 and 5% PTFE samples observed using AFM. The error bars depict the standard error of the mean. *t*-Tests show significant differences such that *p < 0.05 and ***p < 0.001.

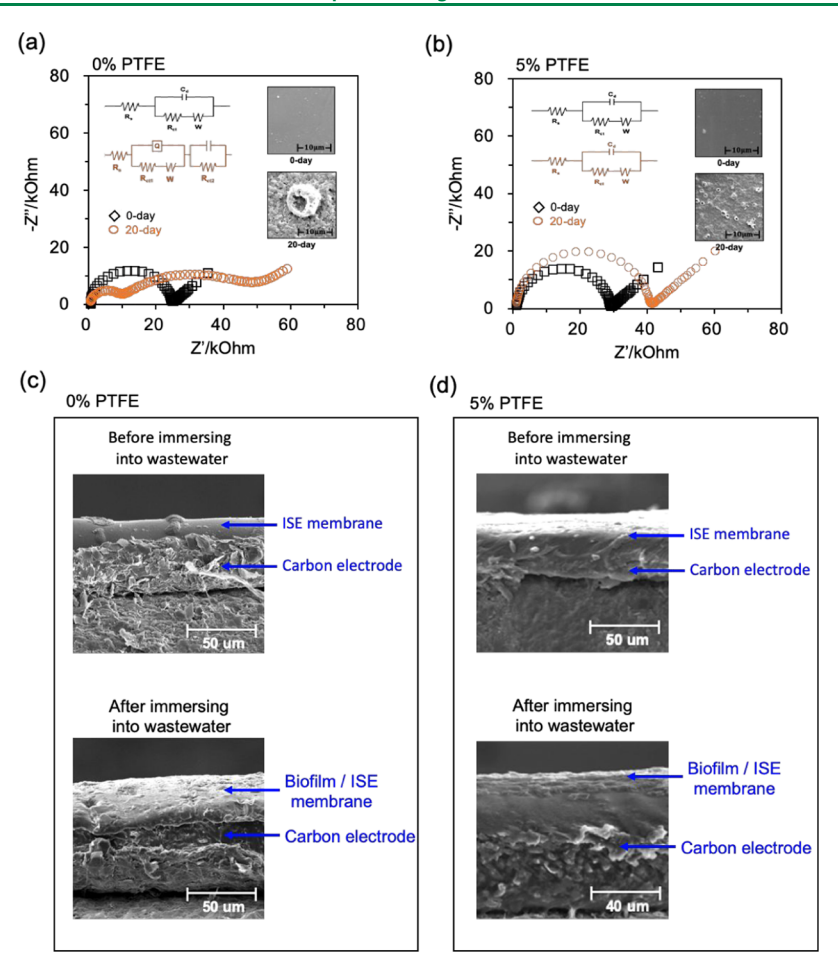


Figure 6. Impedance analysis of NO₃⁻ S-ISEs with 0% PTFE (a) and 5% PTFE (b) before and after 20 days in wastewater. (The inset schematics in (a) and (b) depict the corresponding equivalent circuit diagram models, while the inset images in (a) and (b) present the secondary electron images from an SEM for the sensor surfaces pre and post testing.) The cross-sectional SEM images of S-ISEs (0 and 5% PTFE) (c, d) before and after 20 days in wastewater.

smoother surface, which effectively prevents bacterial attachment. Furthermore, the skewness values for 0% PTFE S-ISE (Table S4) are significantly further away from 0 than for the 5% PTFE S-ISE membrane (-1.0 ± 0.1 and 0.1 ± 0.1 for S-ISE and 5% PTFE, respectively, with $p = 1.5 \times 10^{-8}$) (Figure 5b), again based on 15 regions per specimen. The strongly negative skewness for the 0% PTFE S-ISE membrane quantifies that the surface structure predominantly exhibits pores or valleys, as opposed to relatively no skewness for the 5% PTFE S-ISE membrane as expected when the topography is equally weighted around the average surface height. The impressive resistance to biofouling by microbial cells in wastewater, demonstrated in Figure S2 for our "slippery" and smooth PTFE-containing NO₃⁻ S-ISEs, results from this combined influence of a fine nanoscale surface roughness²⁵ and strongly negative surface charge over the pH range common to real wastewater.

Electrochemical and Scanning Analysis of Sensor Surface over 20 Days in Wastewater. The long-term stability of NO₃⁻ S-ISEs with 5% PTFE is demonstrated in Figure 1b based on immersing them in real wastewater for 24 days during constant operation. SEM images before and after these experiments, the insets in Figure 6, clearly reveal a smooth initial surface morphology in agreement with the virgin samples studied by AFM (Figures 5 and S10). Following almost 3 weeks in wastewater, on the other hand, reveals high

amounts of bacterial cells in wastewater attached to the surface of the 0% PTFE NO₃⁻ S-ISE (Figure 6a and the expanded image in Figure S11) membrane and much less accumulation for the 5% PTFE NO₃ - S-ISEs (Figure 6b). Compared with the S-ISE membrane before immersion into wastewater (thickness of the membrane: $\sim 20 \mu \text{m}$; Figure 6c), the developing overcoat of microbial cells and other fouling species on the sensor surface without the benefit of the PTFE addition was clearly observed (Figure 6c), explaining the sensitivity loss of the 0% PTFE sensors from -52.43 to -29.23mV/dec after just 7 days (Figure 1c). Individual bacterium aggregates together to form large flocs and blocks the pores of the S-ISE membrane and inhibits the permeability to NO₃ ions. Especially, bacterial cells even penetrate into the membrane polymer matrix and consequently impair the sensor (Figure 6c). Comparatively, the PTFE-containing sensor developed a much less substantial biofilm coating after immersing into the wastewater (Figure 6d), explaining that the sensitivity of the 5% PTFE membrane still sustained better than -50 mV/dec throughout 7 days.

Nyquist plots of electrochemical impedance spectroscopy (EIS) results are in agreement with this explanation. Before immersing in wastewater (0 day), the predominant feature for both sensors is a single semicircle corresponding to the bulk resistance of the S-ISE membrane ($R_{\rm S}$ in the equivalent circuit models). The bulk resistance of 0% PTFE sensors dropped

while a resistive layer becomes visible (Figure 6a), representing two bulk resistances with one from the S-ISE membrane while the other must be from biofilms.⁶⁶ The charge-transfer resistance corresponding to the S-ISE membrane increases from 23.6 to 42.5 k Ω after 20 days, i.e., the ion permeability of the S-ISE membrane diminishes. 67 The accumulating bacteria, eventually forming a dense micelle layer, effectively develop another interface in series 68,69 and explain the additional parallel element of charge-transfer resistance (7.7 k Ω). By contrast, the Nyquist plots for the PTFE-containing S-ISEs (Figure 6b) do not evidence any such additional resistances in the high-frequency range, in fact retaining an identical circuit model. The charge-transfer resistance change is also smaller after 20 days than without PTFE (only from 27.7 to 39.4 k Ω). Together, these results confirm that the very low amount of bacteria attaching to the S-ISE membrane surface did not impede the transmembrane diffusion of NO₃⁻ ions into the S-ISE membrane polymer matrix for detection. The incorporation of PTFE in S-ISEs is therefore effective in improving long-term reliability not just by diminishing water invasion and hence attenuating reading (mV) drifting but also for minimizing biofouling and corresponding sensitivity losses. With only an ~40% loss of sensitivity after 20 days of continuous operation in real wastewater, this is proven electrochemically and visually (SEM), assuring the application of our novel PTFE-incorporating sensor design for long-term, real-time, in situ nitrate monitoring in real-world conditions.

Significance of Using PTFE for Long-Term Continuous Monitoring of Water Quality. We have demonstrated that incorporating 5% of the super-hydrophobic polymer PTFE greatly improves the hydrophobicity of S-ISEs, reducing water invasion into the membrane, while the highly negatively charged and smooth surface effectively repels microbial cells in water supplies. This novel design, for the first time, successfully sustained stable performance in real wastewater for sensing nitrates over 20 days, a promising advance toward viable, longterm, accurate, and continuous monitoring of wastewater quality. Coupled with the miniature sensor size, simple fabrication, easy deployment, and minimal necessary power supply makes PTFE-modified nitrate S-ISEs compelling for real-time in situ monitoring in a wide range of water bodies, even including those with harsher requirements (e.g., groundwater, marine water).

However, there is a limit to the benefits of such a strongly negatively charged sensor. If the surface is too highly hydrophobic, this could pose high resistance for ions to migrate through the S-ISE membrane polymer matrix and furthermore can be susceptible to surface fouling by less negatively or even positively charged species in the water.^{70,71} This is one of the reasons that 5% PTFE is an optimal proportion instead of more PTFE ratios (7.5 and 10%). Furthermore, although the sensitivity of 5% PTFE NO₃ - S-ISEs still retained better than -35 mV/dec after 20 days in wastewater, several strategies could be implemented to improve sensor accuracy and durability in wastewater even further. Data correction models for real-time compensation^{72,73} of the varying sensor sensitivity, ion-permeable antifouling membrane coatings⁷⁴ on the sensor surface, might enable continuous sensing functionality for several months or even 1 year.

CONCLUSIONS

The long-term accuracy and durability of NO₃⁻ S-ISEs for continuous wastewater monitoring have been enhanced by mixing the S-ISE membrane polymer matrix with PTFE $(C_2F_4)_n$ to combine two crucial functions—the water repellency of the S-ISE membrane polymer matrix (to reduce water layer formation) and antifouling sensor surface (to prevent bacterial attachment). The optimal ratio of PTFE in the S-ISE membrane polymer matrix is 5%, according to investigations of the accuracy, sensitivity, and durability in real wastewater. As supported by water layer tests, this is partially because the PTFE effectively minimizes water layer invasion into the sensors. Five percent PTFE-loaded NO₃ S-ISEs furthermore resist biofouling in real wastewater (NO₃concentrations ranging from 15 to 18 mg/L) over 24 days, explained by a higher negative surface charge (-4.5 to -45.8 mV) compared to sensors with 0% PTFE (22.1 to -25.9 mV). According to AFM images and roughness calculations, they exhibit a smoother surface as well. Ultimately, the PTFEloaded NO₃ S-ISEs sustained a sensitivity above -35 mV/dec even after 20 days in wastewater during continuous operation every 5 s, exemplifying long-term accurate and real-time monitoring of nitrate in wastewater via this novel sensor.

ASSOCIATED CONTENT

Supporting Information

The Supporting Information is available free of charge at https://pubs.acs.org/doi/10.1021/acssensors.0c01422.

Constituents of NO₃⁻ S-ISEs with the different ratios (0, 2.5, 5, 7.5, and 10%) of poly(tetrafluoroethylene) (PTFE) powder, the detailed parameters of the discharged wastewater in the UConn Wastewater Treatment Plant, the raw values for arithmetic average roughness in 500 nm square regions of fifteen 0 and 5% PTFE S-ISE sample locations, and the raw values for skewness in 500 nm square regions of fifteen 0 and 5% PTFE S-ISE sample locations (Tables S1-S4); the cross-section SEM images of the carbon-based working electrode, the SEM image of PTFE particles and the average size of PTFE particles, the comparison of data stability between the 5% PTFE nitrate S-ISE and commercial sensor for 25 mins in wastewater, the accuracy validation of the commercial sensor readings, the SEM images of S-ISE membrane with 0% (a), 5% (b), and 10% (c) PTFE, the selectivity of 0 and 5% PTFE-loaded nitrate S-ISE, the adhesion test of solidstate ISE membrane with 0 and 5% PTFE before and after immersing (7-day) in water solution (a) and images of the water contact angle at surfaces of sensors with 0 and 5% PTFE (b), the zeta potential of PTFE powder (a) and the chemical structure of monomer TFE and PTFE molecules (b), the impacts of nitrate concentrations (0.2, 1, 2, 4, 8, and 16 mM) on the surface charge (a, b) of the S-ISEM membrane with 0 and 5% PTFE and the sensitivity variations (c, d), AFMresolved surface topography over 5 μ m \times 5 μ m regions for S-ISE with 0 and 5% PTFE (a, b) and representative 500 nm \times 500 nm images (c, d), the SEM images of surfaces of nitrate S-ISE sensor membranes with 0% PTFE (a) and 5% PTFE (b) before and after a 20 day immersion into wastewater (Figures S1-S11) (PDF)

AUTHOR INFORMATION

Corresponding Author

Baikun Li — Department of Civil & Environmental Engineering, University of Connecticut, Storrs, Connecticut 06269, United States; orcid.org/0000-0002-5623-5912; Phone: 860-486-2339; Email: baikun.li@uconn.edu

Authors

- **Yingzheng Fan** Department of Civil & Environmental Engineering, University of Connecticut, Storrs, Connecticut 06269, United States
- **Yuankai Huang** Department of Civil & Environmental Engineering, University of Connecticut, Storrs, Connecticut 06269, United States
- Will Linthicum Department of Materials Science & Engineering, University of Connecticut, Storrs, Connecticut 06269, United States
- Fangyuan Liu Institute of Materials Science, University of Connecticut, Storrs, Connecticut 06269, United States
- André O'Reilly Beringhs School of Pharmacy, University of Connecticut, Storrs, Connecticut 06269, United States
- **Yanliu Dang** Institute of Materials Science, University of Connecticut, Storrs, Connecticut 06269, United States
- **Zhiheng Xu** Department of Civil & Environmental Engineering, University of Connecticut, Storrs, Connecticut 06269, United States
- Shing-Yun Chang Institute of Materials Science and Department of Chemical and Biomedical Engineering, University of Connecticut, Storrs, Connecticut 06269, United States
- Jing Ling Department of Civil & Environmental Engineering, University of Connecticut, Storrs, Connecticut 06269, United States
- Bryan D. Huey Department of Materials Science & Engineering, University of Connecticut, Storrs, Connecticut 06269, United States
- Steven L. Suib Institute of Materials Science, University of Connecticut, Storrs, Connecticut 06269, United States;
 orcid.org/0000-0003-3073-311X
- Anson W. K. Ma Institute of Materials Science and Department of Chemical and Biomedical Engineering, University of Connecticut, Storrs, Connecticut 06269, United States
- Pu-Xian Gao Institute of Materials Science, University of Connecticut, Storrs, Connecticut 06269, United States;
 orcid.org/0000-0002-2132-4392
- Xiuling Lu School of Pharmacy, University of Connecticut, Storrs, Connecticut 06269, United States; o orcid.org/0000-0002-1961-8156
- Yu Lei − Department of Chemical and Biomedical Engineering, University of Connecticut, Storrs, Connecticut 06269, United States; ⑤ orcid.org/0000-0002-0184-0373
- Montgomery T. Shaw Institute of Materials Science, University of Connecticut, Storrs, Connecticut 06269, United States

Complete contact information is available at: https://pubs.acs.org/10.1021/acssensors.0c01422

Notes

The authors declare no competing financial interest.

ACKNOWLEDGMENTS

This study was supported by the National Science Foundation (NSF) Environmental Engineering Program GOALI Project (Grant no.: 1706343), the NSF Partnerships for Innovation (PFI) Accelerate Innovative Research (AIR) Project (Grant no.: 1640701), and Connecticut Biopipeline Program. The project is also partially funded by Infiltrator Water Technologies LLC. W.L. and B.D.H. recognize the support from the UConn Institute of Materials Science, and the AFM is made available via NSF DMR:MRI (Grant no.: 1726862). F.L. and P.-X.G. are grateful to the support by the UConn CARIC Initiative program. The microscopy studies were performed using the facilities in the UConn/Thermo Fisher Scientific Center for Advanced Microscopy and Materials Analysis (CAMMA). S.L.S. acknowledges the support of this research from the National Science Foundation (Grant no.: 1803343). Peter Menard at the Center of Clean Energy Engineering (C2E2) at the University of Connecticut provided his help for transmittance measurement.

REFERENCES

- (1) Park, Y.; Park, S.; Nguyen, V. K.; Yu, J.; Torres, C. I.; Rittmann, B. E.; Lee, T. Complete Nitrogen Removal by Simultaneous Nitrification and Denitrification in Flat-Panel Air-Cathode Microbial Fuel Cells Treating Domestic Wastewater. *Chem. Eng. J.* **2017**, *316*, 673–679.
- (2) Khanfar, M. F.; Al-Faqheri, W.; Al-Halhouli, A. Low Cost Lab on Chip for the Colorimetric Detection of Nitrate in Mineral Water Products. *Sensors* **2017**, *17*, No. 2345.
- (3) Bouvier, J. C.; Bekri, M.; Mazouni, D.; Schoefs, O.; Harmand, J.; Ribeiro, T.; Pham, H. N.; Pauss, A. On-Line Monitoring of Nitrate and Nitrite by UV Spectrophotometry in a SBR Process Used for the Treatment of Industrial Wastewaters. *Int. J. Chem. React. Eng.* **2008**, *6*, 1542–6580.
- (4) Basaglia, M.; Toffanin, A.; Baldan, E.; Bottegal, M.; Shapleigh, J. P.; Casella, S. Selenite-Reducing Capacity of the Copper-Containing Nitrite Reductase of *Rhizobium sullae*. FEMS Microbiol. Lett. **2007**, 269, 124–130.
- (5) Quan, D.; Nagarale, R. K.; Shin, W. A Nitrite Biosensor Based on Coimmobilization of Nitrite Reductase and Viologen-Modified Polysiloxane on Glassy Carbon Electrode. *Electroanalysis* **2010**, *22*, 2389–2398.
- (6) Alahi, M. E. E.; Mukhopadhyay, S. C.; Burkitt, L. Imprinted Polymer Coated Impedimetric Nitrate Sensor for Real-Time Water Quality Monitoring. Sens. Actuators, B 2018, 259, 753–761.
- (7) Campos, I.; Masot, R.; Alcañiz, M.; Gil, L.; Soto, J.; Vivancos, J. L.; García-Breijo, E.; Labrador, R. H.; Barat, J. M.; Martínez-Mañez, R. Accurate Concentration Determination of Anions Nitrate, Nitrite and Chloride in Minced Meat Using a Voltammetric Electronic Tongue. Sens. Actuators, B 2010, 149, 71–78.
- (8) Mani, V.; Periasamy, A. P.; Chen, S. M. Highly Selective Amperometric Nitrite Sensor Based on Chemically Reduced Graphene Oxide Modified Electrode. *Electrochem. Commun.* **2012**, 17, 75–78.
- (9) Huang, Y.; Wang, T.; Xu, Z.; Hughes, E.; Qian, F.; Lee, M.; Fan, Y.; Lei, Y.; Bru, C.; Li, B. Real-Time in Situ Monitoring of Nitrogen Dynamics in Wastewater Treatment Processes Using Wireless, Solid-State, and Ion-Selective Membrane Sensors. *Environ. Sci. Technol.* **2019**, *53*, 3140–3148.
- (10) Perez, M. D. L. A. A.; Florian, K. Y. N. A New Potentiometric Sensor for Nitrate Using Diethylphthalate (DEP) as Plasticizer and Triocthylmethylammonium Chloride (TOMACI) as Ionophore. *Rev. Cubana Quim.* **2018**, *30*, 277–288.
- (11) Yang, S.; Wo, Y.; Meyerhoff, M. E. Polymeric Optical Sensors for Selective and Sensitive Nitrite Detection Using Cobalt(III)

- Corrole and Rhodium(III) Porphyrin as Ionophores. *Anal. Chim. Acta* 2014, 843, 89–96.
- (12) Yang, S.; Meyerhoff, M. E. Study of Cobalt(III) Corrole as the Neutral Ionophore for Nitrite and Nitrate Detection via Polymeric Membrane Electrodes. *Electroanalysis* **2013**, *25*, 2579–2585.
- (13) Fan, Y.; Xu, Z.; Huang, Y.; Wang, T.; Zheng, S.; Depasquale, A.; Brüeckner, C.; Lei, Y.; Li, B. Long-Term Continuous and Real-Time in Situ Monitoring of Pb (II) Toxic Contaminants in Wastewater Using Solid-State Ion Selective Membrane (S- ISM) Pb and PH Auto-Correction Assembly. J. Hazard. Mater. 2020, 400, No. 123299.
- (14) Parra, E. J.; Crespo, G. A.; Riu, J.; Ruiz, A.; Rius, F. X. Ion-Selective Electrodes Using Multi-Walled Carbon Nanotubes as Ionto-Electron Transducers for the Detection of Perchlorate. *Analyst* **2009**, *134*, 1905–1910.
- (15) Mousavi, Z.; Bobacka, J.; Lewenstam, A.; Ivaska, A. Poly(3,4-Ethylenedioxythiophene) (PEDOT) Doped with Carbon Nanotubes as Ion-to-Electron Transducer in Polymer Membrane-Based Potassium Ion-Selective Electrodes. *J. Electroanal. Chem.* **2009**, *633*, 246–252.
- (16) Manica, D. P.; Mitsumori, Y.; Ewing, A. G. Characterization of Electrode Fouling and Surface Regeneration for a Platinum Electrode on an Electrophoresis Microchip. *Anal. Chem.* **2003**, *75*, 4572–4577.
- (17) Roodenko, K.; Hinojos, D.; Hodges, K. L.; Veyan, J.-F.; Chabal, Y. J.; Clark, K.; Katzir, A.; Robbins, D. In Non-Dispersive Infrared (NDIR) Sensor for Real-Time Nitrate Monitoring in Wastewater Treatment, Proceedings of Optical Fibers and Sensors for Medical Diagnostics and Treatment Applications XIX, 2019; Vol. 10872.
- (18) Zhu, Z.; Jiang, J.; Wang, X.; Huo, X.; Xu, Y.; Li, Q.; Wang, L. Improving the Hydrophilic and Antifouling Properties of Polyvinylidene Fluoride Membrane by Incorporation of Novel Nanohybrid GO@SiO₂ Particles. *Chem. Eng. J.* **2017**, 314, 266–276.
- (19) Garcia-Ivars, J.; Iborra-Clar, M. I.; Alcaina-Miranda, M. I.; Mendoza-Roca, J. A.; Pastor-Alcañiz, L. Surface Photomodification of Flat-Sheet PES Membranes with Improved Antifouling Properties by Varying UV Irradiation Time and Additive Solution PH. *Chem. Eng. J.* **2016**, 283, 231–242.
- (20) Harsányi, G. Polymer Films in Sensor Applications: A Review of Present Uses and Future Possibilities. Sens. Rev. 2000, 20, 98–105.
- (21) EPA. Estimation Program Interface (EPI) Suite, version 4.0; U.S. Environmental Protection Agency, 2009.
- (22) Weiß, K.; Worn, H. In *The Working Principle of Resistive Tactile Sensor Cells*, IEEE International Conference on Mechatronics and Automation, ICMA, 2005; pp 471–476.
- (23) Katti, V. R.; Debnath, A. K.; Gadkari, S. C.; Gupta, S. K.; Sahni, V. C. Passivated Thick Film Catalytic Type H2 Sensor Operating at Low Temperature. Sens. Actuators, B 2002, 84, 219–225.
- (24) Pauling, L. The Nature of the Chemical Bond. IV. The Energy of Single Bonds and the Relative Electronegativity of Atoms. *J. Am. Chem. Soc.* **1932**, *54*, 3570–3582.
- (25) Wypych, G. Handbook of Antiblocking, Release, and Slip Additives; ChemTec Publishing, 2014.
- (26) Chen, F.; Guo, J.; Xu, D.; Yan, F. Thermo- and PH-Responsive Poly(Ionic Liquid) Membranes. *Polym. Chem.* **2016**, *7*, 1330–1336.
- (27) Fibbioli, M.; Morf, W. E.; Badertscher, M.; De Rooij, N. F.; Pretsch, E. Potential Drifts of Solid-Contacted Ion-Selective Electrodes Due to Zero-Current Ion Fluxes through the Sensor Membrane. *Electroanalysis* **2000**, *12*, 1286–1292.
- (28) Hambly, B.; Guzinski, M.; Pendley, B.; Lindner, E. Evaluation, Pitfalls and Recommendations for the "Water Layer Test" for Solid Contact Ion-Selective Electrodes. *Electroanalysis* **2020**, 32, 781–791.
- (29) Guo, J.; Farid, M. U.; Lee, E. J.; Yan, D. Y. S.; Jeong, S.; Kyoungjin An, A. Fouling Behavior of Negatively Charged PVDF Membrane in Membrane Distillation for Removal of Antibiotics from Wastewater. *J. Membr. Sci.* **2018**, *551*, 12–19.
- (30) Cheng, S.; Oatley, D. L.; Williams, P. M.; Wright, C. J. Positively Charged Nanofiltration Membranes: Review of Current Fabrication Methods and Introduction of a Novel Approach. *Adv. Colloid Interface Sci.* **2011**, *164*, 12–20.

- (31) Hoang, T.; Stevens, G.; Kentish, S. The Effect of Inorganic Electrolytes on the Zeta Potential of Reverse Osmosis Membranes. *Int. J. Chem. Eng.* **2009**, 163.
- (32) Bhattacharjee, S. DLS and Zeta Potential What They Are and What They Are Not? *J. Controlled Release* **2016**, 235, 337–351.
- (33) O'brien, R. W.; Cannon, D. W.; Rowlands, W. N. Electroacoustic Determination of Particle Size and Zeta Potential. *J. Colloid Interface Sci.* **1995**, 173, 406–418.
- (34) Ye, Q.; Keresztes, Z.; Horvai, G. Characterization of the Outmost Surface of Ion-Selective Solvent Polymeric PVC Membranes and Protein Adsorption. *Electroanalysis* **1999**, *11*, 729–734.
- (35) Akin, O.; Temelli, F. Probing the Hydrophobicity of Commercial Reverse Osmosis Membranes Produced by Interfacial Polymerization Using Contact Angle, XPS, FTIR, FE-SEM and AFM. *Desalination* **2011**, 278, 387–396.
- (36) Minami, T.; Sasaki, Y.; Minamiki, T.; Wakida, S.-i.; Kurita, R.; Niwa, O.; Tokito, S. Selective Nitrate Detection by an Enzymatic Sensor Based on an Extended-Gate Type Organic Field-Effect Transistor. *Biosens. Bioelectron.* **2016**, *81*, 87–91.
- (37) Sagle, A. C.; Van Wagner, E. M.; Ju, H.; McCloskey, B. D.; Freeman, B. D.; Sharma, M. M. PEG-Coated Reverse Osmosis Membranes: Desalination Properties and Fouling Resistance. *J. Membr. Sci.* **2009**, 340, 92–108.
- (38) Coma, M.; Puig, S.; Balaguer, M. D.; Colprim, J. The Role of Nitrate and Nitrite in a Granular Sludge Process Treating Low-Strength Wastewater. *Chem. Eng. J.* **2010**, *164*, 208–213.
- (39) Kouba, V.; Vejmelkova, D.; Proksova, E.; Wiesinger, H.; Concha, M.; Dolejs, P.; Hejnic, J.; Jenicek, P.; Bartacek, J. High-Rate Partial Nitritation of Municipal Wastewater after Psychrophilic Anaerobic Pretreatment. *Environ. Sci. Technol.* **2017**, *51*, 11029–11038.
- (40) Mahmoudian, M. R.; Alias, Y.; Basirun, W. J.; Mengwoi, P.; Jamali-Sheini, F.; Sookhakian, M.; Silakhori, M. A Sensitive Electrochemical Nitrate Sensor Based on Polypyrrole Coated Palladium Nanoclusters. J. Electroanal. Chem. 2015, 751, 30–36.
- (41) Oberdisse, J. Aggregation of Colloidal Nanoparticles in Polymer Matrices. *Soft Matter* **2006**, *2*, 29–36.
- (42) Sundfors, F.; Höfler, L.; Gyurcsányi, R. E.; Lindfors, T. Influence of Poly(3-Octylthiophene) on the Water Transport Through Methacrylic-Acrylic Based Polymer Membranes. *Electroanalysis* **2011**, 23, 1769–1772.
- (43) Lindfors, T.; Sundfors, F.; Höfler, L.; Gyurcsányi, R. E. FTIR-ATR Study of Water Uptake and Diffusion through Ion-Selective Membranes Based on Plasticized Poly(Vinyl Chloride). *Electroanalysis* **2009**, *21*, 1914–1922.
- (44) Ping, J.; Wang, Y.; Wu, J.; Ying, Y. Development of an All-Solid-State Potassium Ion-Selective Electrode Using Grapheme as the Solid-Contact Transducer. *Electrochem. Commun.* **2011**, *13*, 1529–1532.
- (45) Veder, J. P.; De Marco, R.; Clarke, G.; Chester, R.; Nelson, A.; Prince, K.; Pretsch, E.; Bakker, E. Elimination of Undesirable Water Layers in Solid-Contact Polymeric Ion-Selective Electrodes. *Anal. Chem.* **2008**, *80*, 6731–6740.
- (46) Sundfors, F.; Lindfors, T.; Höfler, L.; Bereczki, R.; Gyurcsányi, R. E. FTIR-ATR Study of Water Uptake and Diffusion through Ion-Selective Membranes Based on Poly(Acrylates) and Silicone Rubber. *Anal. Chem.* **2009**, *81*, 5925–5934.
- (47) Ewoldt, R. H.; Johnston, M. T.; Caretta, L. M. Experimental Challenges of Shear Rheology: How to Avoid Bad Data. *Complex Fluids in Biological Systems*; Springer, 2015; pp 207–241.
- (48) Tamai, Y.; Aratani, K. Experimental Study of the Relation between Contact Angle and Surface Roughness. J. Phys. Chem. A 1972, 76, 3267–3271.
- (49) Huh, C.; Mason, S. G. Effects of Surface Roughness on Wetting (Theoretical). J. Colloid Interface Sci. 1977, 60, 11–38.
- (50) Wenzel, R. N. Resistance of Solid Surfaces to Wetting by Water. *Ind. Eng. Chem.* **1936**, 28, 988–994.
- (51) Cassie, A. B. D.; Baxter, S. Wettability of Porous Surfaces. *Trans. Faraday Soc.* **1944**, *40*, 546–551.

- (52) Zita, A.; Hermansson, M. Effects of Ionic Strength on Bacterial Adhesion and Stability of Flocs in a Wastewater Activated Sludge System. *Appl. Environ. Microbiol.* **1994**, *60*, 3041–3048.
- (53) Marshall, K. C. Interfaces in Microbial Ecology. 1976. Soil Sci. 1977. 123, 344.
- (54) Abdel-khalek, N. A.; Selim, K. A.; Amir, A.; Farahat, M. M.; Elhendawy, H. H. Enhancement of Selective Bioflocculation of (Quartz-Pyrolusite-Hematite) System Using *Paenibacillus polymyxa* Bacteria. *Bio Technol.* **2015**, *89*, 36712–36717.
- (55) Soni, K. A.; Balasubramanian, A. K.; Beskok, A.; Pillai, S. D. Zeta Potential of Selected Bacteria in Drinking Water When Dead, Starved, or Exposed to Minimal and Rich Culture Media. *Curr. Microbiol.* **2008**, *56*, 93–97.
- (56) Dobbins, S. C.; McGrath, D. E.; Bernards, M. T. Nonfouling Hydrogels Formed from Charged Monomer Subunits. *J. Phys. Chem. B* **2012**, *116*, 14346–14352.
- (57) Wu, L.; Jasinski, J.; Krishnan, S. Carboxybetaine, Sulfobetaine, and Cationic Block Copolymer Coatings: A Comparison of the Surface Properties and Antibiofouling Behavior. *J. Appl. Polym. Sci.* **2012**, *124*, 2154–2170.
- (58) Hobbs, C.; Hong, S.; Taylor, J. Effect of Surface Roughness on Fouling of RO and NF Membranes during Filtration of a High Organic Surficial Groundwater. *J. Water Supply: Res. Technol.*—AQUA **2006**, 55, 559–570.
- (59) Zhong, Z.; Li, D.; Zhang, B.; Xing, W. Membrane Surface Roughness Characterization and Its Influence on Ultrafine Particle Adhesion. *Sep. Purif. Technol.* **2012**, *90*, 140–146.
- (60) Kochkodan, V.; Johnson, D. J.; Hilal, N. Polymeric Membranes: Surface Modification for Minimizing (Bio)Colloidal Fouling. *Adv. Colloid Interface Sci.* **2014**, *206*, 116–140.
- (61) Rana, D.; Matsuura, T. Surface Modifications for Antifouling Membranes. Chem. Rev. 2010, 110, 2448–2471.
- (62) Lee, S. H.; Hong, T. I.; Kim, B.; Hong, S.; Park, H. D. Comparison of Bacterial Communities of Biofilms Formed on Different Membrane Surfaces. *World J. Microbiol. Biotechnol.* **2014**, 30, 777–782.
- (63) Chowdhury, M. R.; Steffes, J.; Huey, B. D.; McCutcheon, J. R. 3D Printed Polyamide Membranes for Desalination. *Science* **2018**, 361, 682–686.
- (64) Zhao, C.; Xu, X.; Chen, J.; Yang, F. Effect of Graphene Oxide Concentration on the Morphologies and Antifouling Properties of PVDF Ultrafiltration Membranes. *J. Environ. Chem. Eng.* **2013**, *1*, 349–354.
- (65) Jhaveri, J. H.; Patel, C. M.; Murthy, Z. V. P. Preparation, Characterization and Application of GO-TiO2/PVC Mixed Matrix Membranes for Improvement in Performance. *J. Ind. Eng. Chem.* **2017**, *52*, 138–146.
- (66) Baranitharan, E.; Khan, M. R.; Prasad, D. M. R.; Teo, W. F. A.; Tan, G. Y. A.; Jose, R. Effect of Biofilm Formation on the Performance of Microbial Fuel Cell for the Treatment of Palm Oil Mill Effluent. *Bioprocess Biosyst. Eng.* **2015**, 38, 15–24.
- (67) Chahal, N.; Siddique, R.; Rajor, A. Influence of Bacteria on the Compressive Strength, Water Absorption and Rapid Chloride Permeability of Fly Ash Concrete. *Constr. Build. Mater.* **2012**, 28, 351–356
- (68) Siu, C. P. B.; Chiao, M. A Microfabricated PDMS Microbial Fuel Cell. J. Microelectromech. Syst. 2008, 17, 1329–1341.
- (69) Zhao, Z.; Shi, S.; Cao, H.; Li, Y. Electrochemical Impedance Spectroscopy and Surface Properties Characterization of Anion Exchange Membrane Fouled by Sodium Dodecyl Sulfate. *J. Membr. Sci.* **2017**, *530*, 220–231.
- (70) Hilal, N.; Ogunbiyi, O. O.; Miles, N. J.; Nigmatullin, R. Methods Employed for Control of Fouling in MF and UF Membranes: A Comprehensive Review. *Sep. Sci. Technol.* **2005**, *40*, 1957–2005.
- (71) Maximous, N.; Nakhla, G.; Wan, W. Comparative Assessment of Hydrophobic and Hydrophilic Membrane Fouling in Wastewater Applications. *J. Membr. Sci.* **2009**, 339, 93–99.

- (72) Yan, K.; Zhang, D. Correcting Instrumental Variation and Time-Varying Drift: A Transfer Learning Approach with Autoencoders. *IEEE Trans. Instrum. Meas.* **2016**, *65*, 2012–2022.
- (73) Zhang, D.; Guo, D.; Yan, K.; Zhang, D.; Guo, D.; Yan, K. A Transfer Learning Approach for Correcting Instrumental Variation and Time-Varying Drift. *Breath Analysis for Medical Applications*; Springer, 2017; pp 137–156.
- (74) Shi, Q.; Su, Y.; Zhao, W.; Li, C.; Hu, Y.; Jiang, Z.; Zhu, S. Zwitterionic Polyethersulfone Ultrafiltration Membrane with Superior Antifouling Property. J. Membr. Sci. 2008, 319, 271–278.